UNIVERSITÀ DEGLI STUDI DI PADOVA

DIPARTIMENTO DI BIOLOGIA

Corso di Laurea magistrale in *Molecular Biology*

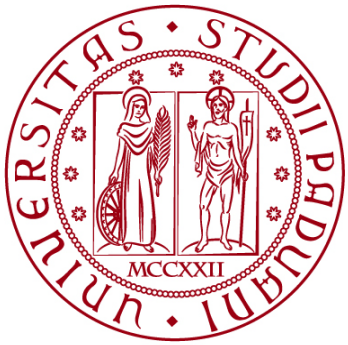

TESI DI LAUREA

Respirometric characterization of mETC mutants and testing of ROS detection assays in the bryophytes model *Physcomitrium patens*

Relatore**: Prof.** ***Tomas Morosinotto***
Dipartimento di Biologia

Laureando**:** ***Matteo Soldera***

ANNO ACCADEMICO 2022/2023

Abstract

This master thesis presents partial physiological characterization of mitochondrial mutants within the moss Physcomitrium patens, employing respirometry data and assessing assays for detecting reactive oxygen species (ROS). The studies implemented, showcase differences in the AOX pathway capacity between the protonema and gametophore stages. In particular protonema tissue is able to carry out respiration when complex IV is blocked by cyanide, utilizing the alternative terminal oxidase AOX. Instead, gametophores shown an increased sensibility to inhibition in respect to protonema. The respirometry analysis carried out on mutants showcase: an increased rate of respiration in complex 4 ko line, confirmed that the respiration detectable in aox deficent line was carried out by complex 4 and the opposite in complex IV ko line. Furthermore, the thesis explores the efficacy of assays designed to detect reactive oxygen species. Results indicate that the tested assays may not be optimal for the unique physiological context of Physcomitrium patens. This finding emphasizes the importance of tailored approaches when studying ROS in moss species and raises critical considerations for future research methodologies.

Table of contents

Abstract 2

Introduction

Chloroplasts and mitochondria, the bioenergetic organelles of plants 5

Why study plant respiration ? 6

The aerobic respiration process in plants 7

The mitochondrial electron transport chain 9

The moss *Physcomitrella patens* 10

Aim of the thesis 11

Material and methods

Plant material and conditions 11

Chlorophyll quantification 14

Respirometry 15

Dark adapted state respiration 18

Capacity of Complex IV- and AOX-mediated pathways *19*

Ferrous oxidation-xylenol orange assay (FOX) 19

DAB staining 22

Nitro blue tetrazolium Staining 23

Results

Optimization of ROS measuring protocols in P. patens 23

Colorimetric determination of hydrogen peroxide 25

Respiratory characterization of *P. patens* WT and mutants 27

Comparison protonema-gametophore *27*

Respiratory characterization of cox11 and aox mutants *29*

Respiration of dark adapted ETC mutants ***29***

Introduction:

Chloroplasts and mitochondria, the bioenergetic organelles of plants

Two organelles are at the core of the energetic metabolism of plants, chloroplasts and mitochondria The first represent the site where energy in form of light is transformed into reducing equivalents and chemical energy used for carbon fixation. Mitochondria are the main consumers of reducing equivalents. Those are obtained by oxidating photosynthetic products or by various kind of reserves under non autotrophic conditions. Both organelles carry out their functions through the use electrons transport chains (ETC) formed by protein complexes and mobile electron carriers. In the chloroplast's ETC of oxygenic photoautotrophs, light energy is absorbed by two different protein complexes, photosystems (PS) I and II. The energy absorbed by the photosystems is used to create a difference in redox potential, by excitation of chlorophyll molecules in the reaction center of the photosystems. The difference in potential is then used within the chloroplast to extract electrons from water (oxidize water), produce reducing equivalents (NAD(P)H) and translocate proton across a membrane to generate an electrochemical potential used for the generation of the energetically dense molecule adenosine triphosphate (ATP). In mitochondria, reducing equivalents that hold a low redox potential (NADH, succinate) are consumed (oxidized) and their electrons streamed through the mitochondrial ETC (mETC). The terminal acceptor of electrons is oxygen, that gets reduced to water. This process generates an electrochemical gradient of protons to generate ATP. The efficiency of the redox reactions in both chloroplasts and mitochondria are strongly influenced by the stoichiometric ratio of the species involved (redox poise) and the local availability of the species. Those reactions involve highly reactive and short-lived species that can easily react outside of the intended pathway and damage cellular components causing a decrease in efficiency of the metabolism.

Mitochondrial function is relevant to photosynthetic function, photorespiratory detoxification, nitrogen and carbon metabolism, environmental and biogenic stress responses. Consequently, understanding better the physiological role of mitochondria

will impact in our ability to improve biomass accumulation and plant resistance to challenging conditions (Millar *et al.*, 2011).

Consistent with the central role in metabolism and being the only source of energy in autotrophic conditions, studying the effects of mutations and change to mETC machinery in spermatophytes has been proven challenging, Spermatophytes present non photosynthetic developmental stages with high demand of energy, this obstacle isolation of mutant with impaired mitochondrial function for the often lethal phenotype of Knock out mutants.

Why study the respiration of plants?

One of the most pressing problems to address for plant biology nowadays it's the plateauing in crop's productivity coupled with increasing population to feed and the depletion of farmable land with increasingly extremes and unstable climate. The maximal photosynthetic efficiencies (light energy absorbed/energy fixed as biomass) for wild type C3 and C4 photosynthesis plant are, respectively, 4.6 and 6.0 % (Zhu, Long and Ort, 2010). Bioengineering of the photosynthetic process to achieve greater efficiency can translate in increased biomass accumulation. The main targets to improve the utilization of light energy by plants are increasing the rate of the chloroplast's electron transport and increasing the allocation of electron to the photochemical pathway, decreasing dissipation. Is also important to make sure that processes consuming the products of photosynthesis can sustains this increased electron transport. Accumulation of products cause excessive reduction of the electron transport chain. Over reduction increase the possibility that electrons react with off target species producing highly reactive molecules like ROS and causing photoinhibition) (Gu, 2023). The products of electrons transport are ATP and NADPH with a ratio of 9 ATP to 7 NADPH when the transport follows the complete pathway from water to NADP+. Those are consumed for CO_2 fixation in the chloroplast with a ratio of 9ATP:6NADPH. To compensate for this disequilibrium plant in the wild utilize different strategies like cyclic transport of electron around photosystem I or exporting

excessive reducing power to the cytoplasm in the form of malate. Mitochondria sustain chloroplasts during photosynthesis participating in the photorespiratory pathway and utilizing the reducing equivalent exported for ATP synthesis and biosynthetic intermediates production, balancing the ratio between ATP and reducing equivalent. They also represent the sink of the products of the CO_2 fixation and are pivotal in the nitrogen metabolism, being crucial for regulating the biomass accumulation.

To sustain an impactful increase in crop's yield, besides the understanding of photosynthesis, a deep knowledge of the functioning and interconnection of the activity of mitochondria must be acquired**.** Respiration is the main metabolic process for which the mitochondria is responsible, studying the physiological effects on the plant of changes in mitochondrial electron transport chain could be a step towards future food stability and maybe a harm reduction of climate crisis and a small bandage for biodiversity loss.

The aerobic respiration process of plants

Aerobic respiration is a process of transformation of chemical energy from oxidable substrates, into reducing equivalents (NADH) and ATP. These species will then be used to carry on biosynthetic pathways.

In plants the respiration process starts in the mitochondrial matrix with the Tricarboxylic acid cycle. Pyruvic acid imported from the cytosol is oxidized to acetyl-CoA thanks to the action of the pyruvate dehydrogenases complex, with the production of CO_2 and reduction of NAD^+ to NADH. The acetyl group provided by acetyl-CoA is condensed with oxalacetate by the enzyme citrate synthase to produce citrate and regenerate free CoA. Citrate is the first substrate of a set of sequential reactions that constitute the citric acid cycle or Krebs cycle. The two carbons introduced in the cycle as acetyl are oxidized to CO_2 and released, the oxalacetate is regenerated and the free energy released by the oxidation reactions is used to produce reducing equivalents in form of NADH. The overall reaction of pyruvate decarboxylation and oxidation can be

summarized as follows, were Q and QH2 are the oxidized and reduced forms of ubiquinone, respectively.

$$CH_3COCOO^- + 4NAD^+ + Q + GDP + P_i + 2H_2O \rightarrow 4NADH + QH_2 + 4H^+ + GTP + 3CO_2$$

The intermediates of the Krebs cycle also participate in a number of other metabolic processes, for example: in dealing with products of photorespiration, providing carbon skeletons for biosynthetic processes and producing organic acids for secretion in the rhizosphere for nitrogen uptake. These processes imply noncyclic flux model and the need of fine regulation in the kinetics of the enzymes involved, carbon can also enter the process from other points in the cycle other than Acetyl-CoA. Figure 1 recapitulates the step of the TCA cycle and the major processes in which its involved in plant's cells (Zhang and Fernie, 2018).

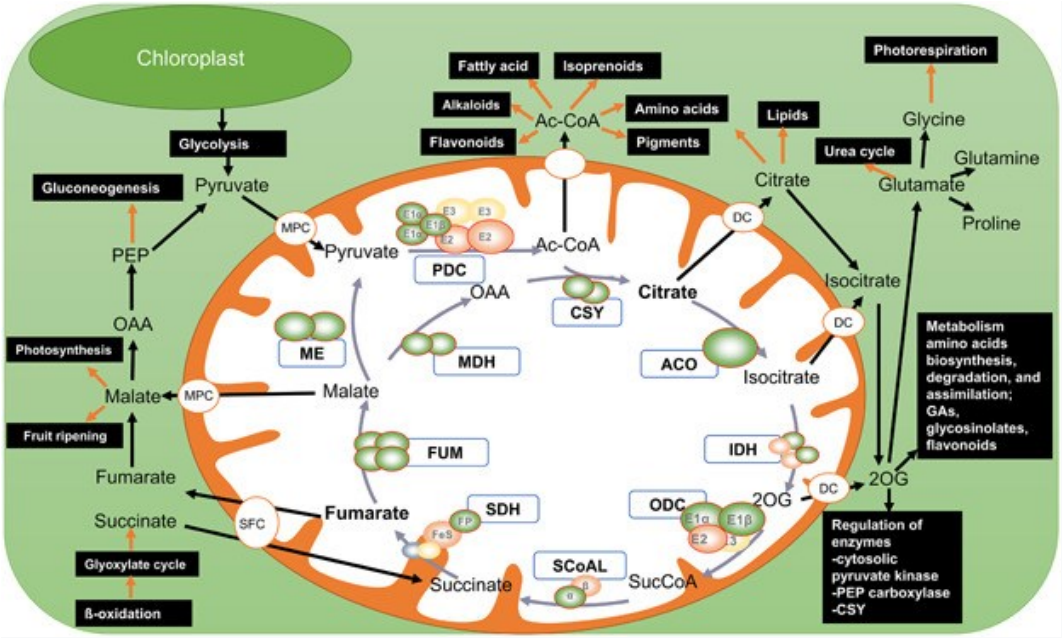

Figure 1. The Krebs cycle blue boxes show the name of the enzymes, green circles represent the subunits of the enzyme, black name are intermediates and blue arrows the reactions. PDC, pyruvate dehydrogenase complex; ME, malic enzyme; CSY, citrate synthase; ACO, aconitase; IDH, isocitratedehydrogenase; ODC, oxoglutarate dehydrogenase complex; SCoAL, succinyl-CoA ligase; SDH, succinatedehydrogenase; FUM, fumarase; MDH, malate dehydrogense; AcCoA, acetyl-CoA; 2OG, 2-oxoglutarate; SucCoA,succinyl-CoA; MPC, mitochondrial pyruvate carrier; SFC, succinate/fumarate carrier; and DC, dicarboxylate carrier. From Zhang and Fernie, 2018.

The mitochondrial electron transport chain of plant

The reducing equivalents produced by the Krebs cycle in the mitochondrial matrix will be oxidized by the mETC to sustain the proton electrochemical potential across the inner mitochondrial membrane, which is used by ATP-synthase to catalyze the phosphorylation of ADP into ATP.

The basic components of the mETC are shared across eukaryotes. These include a set of protein complexes: complex I (NADH:ubiquinone oxidoreductase)), complex II (succinate-ubiquinone oxidoreductase), complex III (coenzyme Q:cytochrome c oxidoreductase), complex IV (cytochrome c oxidase), and complex V (ATP synthase). Complexes I, II and IV couple their oxidoreductase activity with proton translocation across the inner mitochondrial membrane. Together with the protein complexes also mobile electron carriers participate in the process, ubiquinone (or coenzyme Q) and the small Heme containing protein Cytochrome c, which diffuse respectively in the inner membrane lipid bilayer and in the matrix to connect the protein complexes of the ETC. The subunits that can be isolated from each complex of plants mETC (figure 2) differ from the animal's one, for example in plants, up to 49 subunits (cf. 46 in mammals) can be separated from CI by combinations of native and denaturing electrophoresis (Millar *et al.*, 2011) of which 17 are novel subunits only found in plants. The pathway just described, in particular the step of cytochrome C oxidation, can be blocked by cyanide which block the reaction center of complex IV. In addition to the energy conserving path of electron transfer, in plant mitochondria, a cyanide insensitive pathway is present. This pathway bypasses the proton pumping complexes III and IV of the standard chain (complex III oxidize reduced ubiquinone oxidizing cytochrome C, complex 4 oxidize cytochrome C and transfer the electrons to the final acceptor, molecular oxygen, generating water) thanks to a protein that transfers electrons from ubiquinol to oxygen without proton transfer activity, the alternative oxidase (AOX). Also complex I can be bypassed thanks to the action of alternative NAD(P)H dehydrogenases (NDA in Figure 2). AOX appears to play an antioxidant role in plant mitochondria and is encoded by multiple genes in most plants. The expression of the different genes has been shown to be both tissue- and development-specific. Other

components of the alternative pathways involve several type II NAD(P)H dehydrogenases on both sides of the inner membrane. Cytosolic NADH and NADPH can be oxidized via at least two NAD(P)H:UQ oxidoreductases located on the outer surface of the inner membrane. Similar enzymes on the inner side of the membrane enable plant mitochondria to oxidize matrix-produced NAD(P)H. Both pathways operate without the translocation of protons and are often called rotenone-insensitive, or alternative NAD(P)H dehydrogenases. These dehydrogenases are small proteins that transport electrons without conserving the free energy of oxidation and are present in addition to, and compete with, the proton-translocating CI (Type I) NAD(P)H dehydrogenase and SDH (Millar *et al.*, 2011).

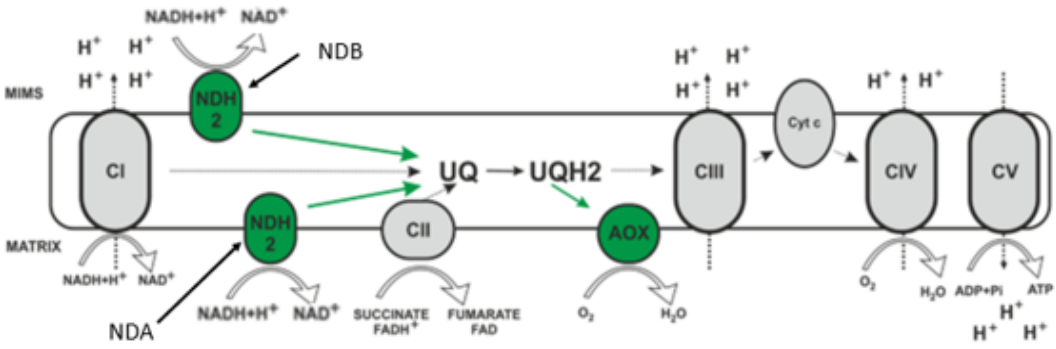

Figure 2: schematic representation of the electron transport chain of plant mitochondria with the bypasses. grey arrows indicate the energy conserving phosphorylating pathway, green arrows indicate the rotenone-cyanide insensitive alternative pathway. CI: complex I, CII: complex II, CIII: complex III, CIV: complex IV, CV: ATP synthase, NDH2: alternative dehydrogenases, AOX: alternative oxydase, Cyt c: cytochrome C, UQ: ubiquinone, UQH2: ubiquinol, H^+: protons. (Catania et al, 2019)

The moss P. patens

The model included in this thesis is the moss *Physchomitrella patens.*

P. patens is a moss exponents of the divison bryophyte. Is used as a model plant for genomics and physiology studies. In nature the plant lives as an ephemeral, germinating from overwintered spores in early summer. It prefers humid conditions, usually developing on ground patch exposed by falling water level on the banks of lakes and river or in damp open field.

As seeds plant and fern, mosses present an alternation of generation with an haploid gametes producing phase (gametophyte) and a diploid spores producing phase (sporophyte). In mosses, contrary to seed plants, the dominant phase of the life cycle is the gametophyte that take the name of protonema.

In *P. patens* spores germinate producing filaments that form the protonema,. Two kinds of filaments are produced, the first formed is composed by densely packed chloroplast rich cells and take the name of chloronema. The second kind of filament produced , caulonema, arise from chloronema, this is composed by faster replicating cell with fewer and less developed chloroplast. Further in the development from side branching of chloronema, "leafy" shoots appear, the gametophores. Those shoots bear gametes producing structures, respectively, Antheridia(male) and archegonia(female). Self-fertilization is possible, and since both structures are carried on the same shoots is also quite common. The male gametes are mobile and needs water to reach the female gamete. After fertilization a zygote is produced, this will develop in a sporophyte dependent on the mother gametophore. The sporophyte at maturation presents a chamber with around 4000 spores obtained by meiosis, that will be released to repeat the cycle. (Cove, 2005).

The fact that the haploid phase is the dominant one, the possibility to vegetatively propagate photosynthetic tissue, together with the high efficiency and relative ease of transformation by homologus recombination, makes *P. patens* an ideal model organism to study effects of mitochondrial mutations.

Aim of the thesis

In this thesis, respirometry and reactive oxygen species assays data acquired in the embryophyte model *Physcomitrium patens* are presented. Knock out mutants of mETC components are included, in particular complex I, complex IV and mitochondrial alternative oxidase knock out obtained from the previous work of (Mellon *et al.*, 2021) and Antoni Vera Vives by homologous recombination mutagenesis.

Material and methods

Plant material and conditions

Several knock out mutant of mitochondrial electron transport complexes are studied in this thesis. The KO mutant have been generated inserting in the nuclear genome of *P. patens,* a gene for antibiotic resistance in the ORF (open reading frame) of the target gene, disrupting the normal translation of the target. The insertion has been obtained through homology mediated recombination of protoplast, a technique with high

efficiency of transformation in *P. patens*(Cove, 2005). The resistance cassete is flanked with sequences homologus to the gene target, spanning around 1000 bp. The complexes targeted where: complex I, complexIV and the alternative oxidase AOX. Since complex I and complex IV comprise of several proteins, genes coding for subunit involved in the correct assembly or positioning of the protein have been targeted (less genetic changes with the most probable success of non-detecting the target complex). For example, in order to stop the production of complex 4 the gene Cox11 have been targeted, this gene code for a chaperon involved in the insertion of copper ions in the catalytic sites of the complex (**inserire citazione disserzione phd di toni).** For the knocking out of complex I two subunits are targeted generating two independent lines; NDUFB10 which constitutes the proton pumping module of the complex, and NDUFB5 that forms part of the module responsible for electron transfer to Ubiquinone. The mutants have been generated and characterized genetically and transcriptionally by the previous work of M. Mellon(Mellon *et al.*, 2021) and A. M. V. Vives (Phd dissertation still unpublished). Also Knock out of the alternative oxidase of mitochondria have been obtained in the same manner.

The genotypic confirmation of the lines has been carried out in the same laboratory where I spent my internship and I have partially participated at the genetic characterization of the *Cox11* deficient line,

The results confirm lack of activity of the target complexes and are published in the works mentioned above so they have not been included in this thesis.

List of mutant lines:

- *ndufa5, ndufb10* → lack complex I activity
- *cox11*→ lacks complex IV activity
- *aox*→ lacks mitochondrial alternative oxidase activity

All mutants and wild type lines used during the experiment were obtained from Gransden ecotype Physcomitrium patens. Plants were cultivated in growth chamber at 22°C, 32% relative humidity with a photoperiod of 16 h\d. Plants were cultivated for 7 days from inoculum in rich medium or 10 days in minimum medium in petri dish. Cellulose filters were placed on top of the medium to avoid penetration of the plants into it and to facilitate subsequent collection. To start a culture protonema was collected with a spatula in sterile condition and transferred to a 15 mL tube containing approximately 4/5 mL of Milli-Q® purified water. The tissue was then homogenized using an Ultra-Turrax® disperser. Around 1\2 mL of homogenate were poured on the petri dish with the solid medium and cellulose filter, unused homogenates were sealed with parafilm and stored at 4°C in the dark. Plants cultivated on minimum media ($PPNO_3$) were used for experimental procedures at the peak of photosynthetic performance for wild type (10 days), instead to propagate and obtain greater amount of tissue for inoculation an enriched version of the media ($PPNH_4$), supplemented with ammonium tartrate and glucose as nitrogen and carbon fonts, was used. A precise recipe for medium is present in Table 1

Table 1: growth media recipes

	[compound]	
COMPOUNDS	***PPNO3***	***PPNH4***
MgSO4 · 7 H2O	0.25 g/L	0.25 g/L
Ca(NO3)2 · 4 H2O	0.80 g/L	0.80 g/L
FeSO4 · 7 H2O	0.0125 g/L	0.0125 g/L
Microelements (1,000 x)	1 mL/L	1 mL/L
phosphate buffer (1,000 x) pH7	1 mL/L	1 mL/L
Ammonium tartrate	–	0.5 g/L
glucose	–	5 g/L
Agar	8 g/L	7.2 g/L
Microelements (1,000 x)		
COMPOUNDS	**[compound]**	
CuSO4 · 5 H2O	5.5 mg/L	
ZnSO4 · 7 H2O	5.5 mg/L	
H3BO3	61.4 mg/L	
MnCl2 · 4 H2O	38.9 mg/L	
CoCl2 · 6 H2O	5.5 mg/L	
KI	2.8 mg/L	
Na2MoO4 · 4 H2O	2.5 mg/L	

Complex I and Complex IV knock out lines were cultivated for longer period (10 days on PPNH4, 14 on PPNO3) due to the very slow and reduced growth phenotype.

To allow gas exchange with the ambient, PPNO3 plates are not completely sealed with Parafilm but partially with Micropore 3M tape., instead PPNH4 plates with the presence of glucose that render carbon not limiting, plates are sealed.

Chlorophyll quantification

All data are normalized to chlorophyll content. After the experimental procedure, sample were recovered and flash freezed in a screw cap 2 mL sardest tube with 3 ceramics balls using liquid nitrogen. Without letting samples defrost 600 uL of 80% v/v Acetone were added to each tube. In the dark, to avoid chlorophyll degradation by light, sample are homogenized using a TissulizerII™ (30Hz, 120 sec.). Homogenizes are then centrifuged at 13.200 G for 3 min. Resulting supernatant is transferred to 1.5

mL Eppendorf and recentrifuged to eliminate debris. 200uL of Chlorophyll extract from each sample are transferred to a 96 wells plate and abs is read at 750nm, 663nm, 645nm and [chl] is then calculated as follow, where OD is the optical density of the media at that wavelength(R.J. Porra and Dioision, 1988):

$$[Chl]\left(\frac{\mu g}{mL}\right) = \{20.20 * [OD(645) - OD(750)] + 8.02 * [OD(663) - OD(750)]\}$$

Respirometry

Since the big part of the data presented in this thesis are oxygen evolution/consumption rate, a description of the theoretical functioning of an oxygen sensor is provided. To measure dissolved oxygen concentration in solution a Polarographic oxygen sensor, or Clark electrode, is used. The sensor is constituted of two electrodes, a gold (or other noble metal like platinum) working cathode and a silver-silver chloride anode which works both as reference electrode and counter anode. All of this is immersed in an electrolyte solution of potassium chloride and the whole system is connected with the measured media in by an Oxygen permeable membrane. Between the two electrodes a polarizing voltage is applied. The polarization voltage must be greater than the standard redox potential (+401 mV) of the reaction at the cathode, but with reversed polarity. At the cathode oxygen is reduced and concomitantly Silver is oxidized at the anode. The rate at which the electrocatalysis proceeds is determined by the polarizing voltage applied, above a certain threshold the current depends solely on the rate at which oxygen can diffuse across the membrane (the reduction of oxygen at cathode create a dynamic concentration differential that drives the oxygen diffusion). Electrons are extracted from silver thanks to the voltage applied. Those arrive at the cathode with higher potential energy and react with molecular oxygen at the surface, the product of the oxygen reduction are ultimately hydroxide ions (OH^-), those diffuse into the electrolyte solution and balance out the charge of the chloride ions (Cl^-), which is consumed by the formation of silver chloride at the anode. Ag^+ produced by the silver oxidation reacts with chlorine ions in solution. This process creates a current trough the circuit that can be measured and is directly correlated to the rate of oxygen diffusion

across the membrane which is directly linked to Oxygen activity in the measuring solution. Normally the rate of diffusion is dependent on the difference between concentrations, but since at the cathode oxygen is practically immediately consumed $[O_2]_{cathode}$ can be considered 0. The solution needs constant stirring in order to maintain the oxygen concentration through the volume. So, converting the amperometric signal into voltage we can derivate the oxygen concentration in solution. (Song and Zhang, 2008)

The semireactions of the species involved are:

$O_2 + 4e^- + 2H_2O \rightarrow 4OH^-$

$Ag \rightarrow Ag^+ + e^-$

The whole redox reaction

$O_2 + 4Ag + 2H_2O \rightarrow 4OH^- + 4Ag^+$

(Fork, 1972). reference (1) (2)

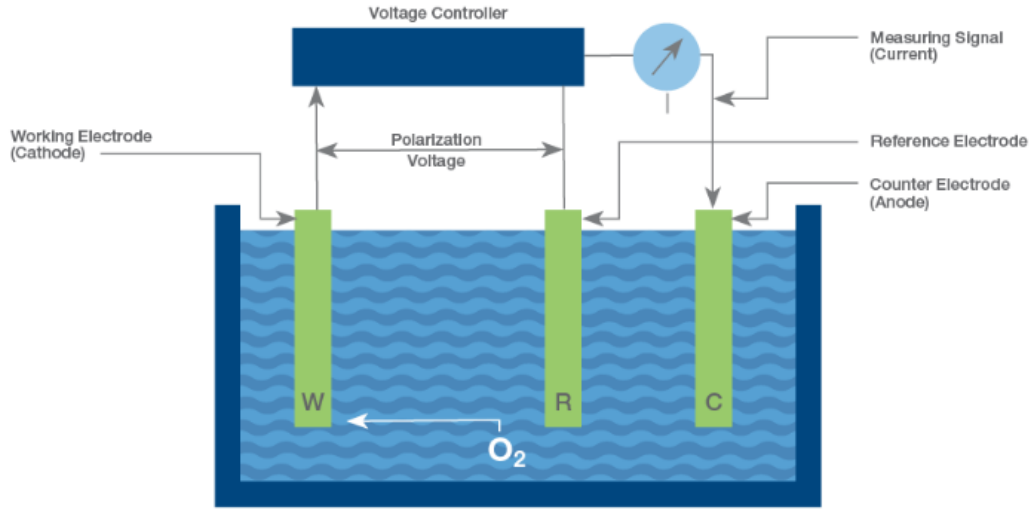

Figure 4: schematic representation of a Clark type sensor with the main functional parts, in real life application all the component are assembled in a much more compact space and efficent way. Sourced from: https://www.hamiltoncompany.com/process-analyt

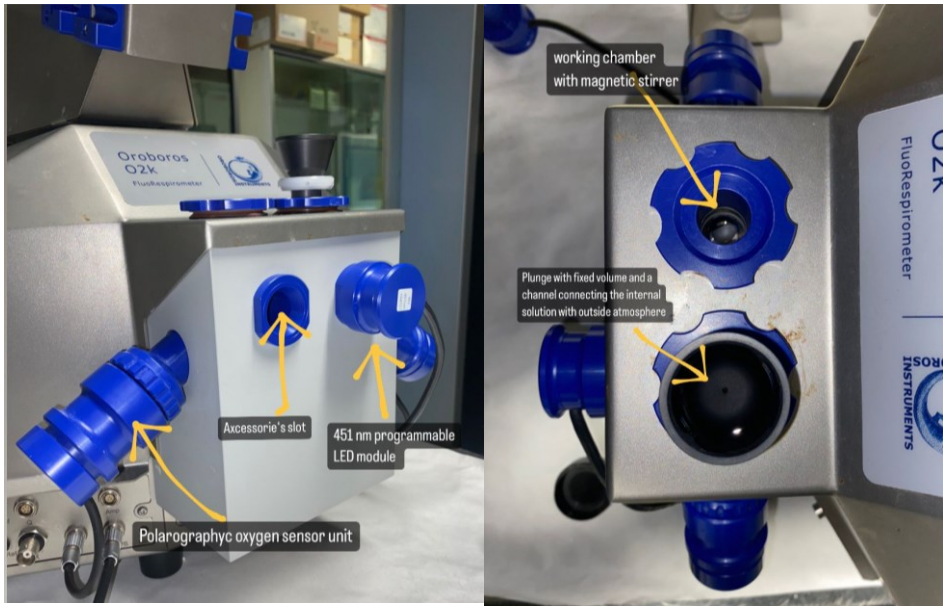

Figure 3: Oroboros system, with main components, used for collection of data presented in this thesis.

All respirometry measures were performed using an Oroboros™ system, the system functioning is based on polarographic oxygen sensors (POS). The whole apparatus consists of 2 fixed volume chambers (2mL) with 1 POS each accessing the working volume. The chambers are filled with the liquid version of PPNO3 + $NaHCO_3$ 100 mM (bicarbonate ion produce CO_2 as part of its equilibrium reaction, carbon not limiting) a magnetic stirring rod mix the solution and a transparent window on the front enable to

expose the samples to light sources. Samples were hold in the middle of the chamber by a metal grid (sample holder). The whole measuring block is kept at 22° C.

The POS cause the reduction of molecular oxygen at the surface of the working cathode paring it with the oxidation of silver metal at the anode, to make the reactions happen a voltage equal and of inverse polarity of the standard redox potential of the oxygen reduction must be applied, the resulting current generated will be proportional to the rate of Oxygen reduction which is directly linked to oxygen concentration in solution through the diffusion constant of oxygen across a selective membrane. The amperometric measure is then converted to an oxygen flux track ($\partial[O_2]/\partial t$, pmol O_2*sec^{-1}) and into absolute Oxygen concentration (mmol) track (across time)

All measurement were then normalized on chlorophyll content of the sample.

Dark adapted state respiration

This set of experiment consisted in measuring the oxygen consumption rate (pmol O_2\s) of plants in dark adapted state. Plates with the selected genotype are taken from the growth chamber and coated with aluminum foil for 40 min, from this point on all operation are done in the dark. Material sufficient to create a small ball of ≈ 0.5 cm is picked up using a spatula and carefully positioned on the sample holder inside the measuring chamber. The chamber is closed and, after attending equilibration with the atmosphere, the oxygen consumption rate is measured as the median of a track segment spanning around 60 seconds just before light turning on (figure5 show an example of a selected segment).

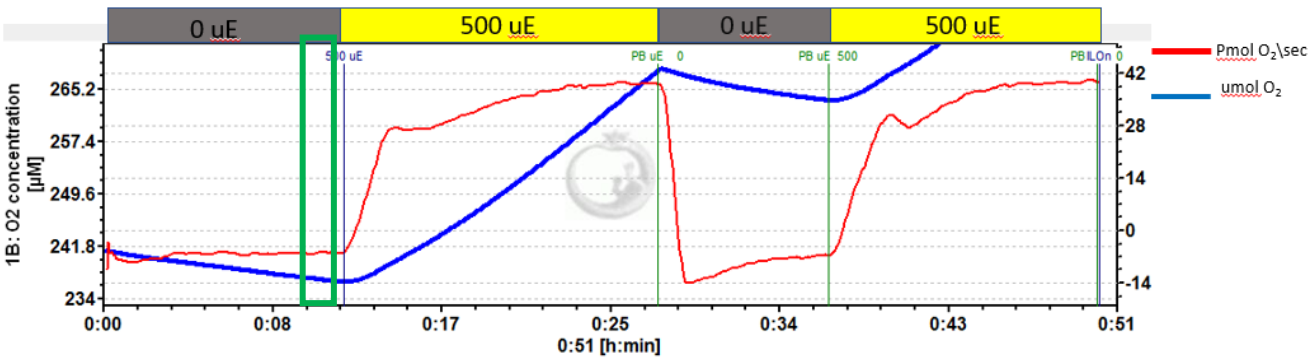

Figure 5: oxygen flux and oxygen concentration tracks from respirometric analysis of 10 days old wildtype protonema exposed to two cycle of illumination (upper boxes indicate light intensity) the green box rappresent an example of analyzed segment.

Capacity of Complex IV- and AOX-mediated pathways

The effects on oxygen consumption of application of single or pair of mETC inhibitors was assessed, in particular the inhibitors tested were: potassium cyanide (KCN), which inhibits complex IV, and Salicylhydroxamic acid (SHAM), which inhibits AOX. inhibitors with the same targets of previous were tested to check that the observed effect was dependent on mETC component inhibition and no other confounding effects (antimicin A complex IV inhibitor, n-propil gallate AOX inhibitor), there was no observable difference, so experiments proceeded with KCN and SHAM who were more abundant and less costly.

Sample are inserted in the measuring chamber as described before and after the dark-adapted respiration rate is measured either 4 uL of KCN 0.5 M or 8 uL of SHAM 0.250 M are added using a micro syringe, for a final concentration of 1 mM. Due to the slight change in media composition the signal is very unstable right after the addiction, the new oxygen consumption is measured (as before) after the signal become stable for some consecutive minutes. Then the second inhibitor is add, and the measurement performed in the same manner as the first.

Ferrous oxidation-xylenol orange assay (FOX)

FOX assay is a colorimetric protocol to measure the concentration of hydrogen peroxide in an aqueous extract of plants tissue. The assay is based on the oxidation of

ferrous ions to ferric ions in acidic condition and further oxidation of xylenol orange. Absorbance is then fitted to a standard function calculated on standard solutions. Three solutions are prepared under ice and avoiding light exposition:

-Solution A: 0.49 g Ammonium iron (II) sulfate ($(NH_4)_2Fe(SO_4)_2(H_2O)_6$) in 50 mL sulfuric acid (H_2SO_4) 2.5 M

-Solution B: 0.0047 g of Xylenol Orange tetrasodium salt (CAS number 3618-43-7), 0.9100 g D-sorbitol, 500 uL ethanol (CH_3CH_2OH) to 50 mL with ultrapure water.

-Grinding Buffer: potassium phosphate buffer 0.1 M 6.4 pH + potassium cyanide (KCN) 0.5 mM

When all solutions are ready, standards are prepared as follows. A stock solution of known concentration of hydrogen peroxide is diluted in ultrapure water to obtain a ≈ 60,0 uM mother solution. Serial dilution (1:2) is used to obtain 8 standards ranging from $[H_2O_2]$ =0 to the mother solution concentration. All standard concentration must be precisely known. Independent technical replicate must be produced (at least 2 points for concentration). Once all the solution are ready samples can be collected, each sample should be collected in the conditions of interest since peroxide degradation is quite fast, around 25 mg of protonema are picked up with a spatula and gently dried with absorbent paper, fresh weight is registered, and the sample is flash frozen with liquid hydrogen in a 1.5 mL centrifuge tube. 500 uL of grinding buffer are added to each sample and, while frozen, sample are finely grinded for 1 minute using a mortar to extract the cellular contents. After grinding extracts are centrifuged for 2 min at 14000 rpm.

To perform the analysis 500uL of solution A are added to solution B to create the Fox reagent (Fr), 150 uL are added to individual dwell in a 96 dwells Sardest™ plate and 15 uL of standard solution or sample's extract are added on top of Fr. The plate is then loaded in a Spark® multimode microplate reader, shacked for 10 seconds, incubated at room temperature for 40 minutes and then optical density is measured at 800 nm and 550 nm. A standard curve is produced graphing the difference in optical density (OD_{550} – OD_{800}) against the standard concentration and then fitting a linear function to them.

From the function fitted to the standard's points parameters are derived to calculate $[H_2O_2]$ in sample's extracts from theirs $OD_{550} - OD_{800}$.

From standard, if $x=(OD_{550} - OD_{800})$ we obtain a function of the kind:

$f(x)=mx + q$

$f(x)=[H_2O_2]$

$[H_2O_2]_{sample}=m(OD_{550} - OD_{800})_{sample}+q$

From the fitted function we know the parameters *m* and *q* and we can then use the known $OD_{550} - OD_{800}$ of sample's extracts to estimate the peroxide concentration in them.

DAB staining

3,3′-Diaminobenzidine (DAB) is a water-soluble organic compound that reacts with hydrogen peroxide in the presence of iron containing enzymes to produce a dark brown precipitate. To obtain qualitative information on hydrogen peroxide content in different mETC mutants and in plants subjected to different growth conditions, protonema and gametophores samples were stained with DAB. Pictures taken with a Leica EZ4W stereomicroscope. The protocol used is based on the Arabidopsis staining protocol reported by (Daudi and O'Brien, 2012).

Tissue samples of both protonema and gametophores are collected from PPNO3 plates using a spatula and a tweezer, paying attention not to collect growth medium with them. The collected samples are stained in a suitable container with a solution 1.0 mg/mL DAB + 0.05% (v\v) Tween™ 20 in phosphate buffer 75 mM pH 7 in the dark for 2 hours. After the staining, samples are retrieved and incubated for 20 minutes at 95 °C in a 3:1:1 mixture of ethanol, acetic acid, and glycerol to remove pigments and obtain a transparent sample. Samples, if not imaged right after, are stored at 4 °C in the mixture just described up to 4 days. To image stained samples, those are placed on a glass slide in a monolayer with the help of the mixture and observed at the stereomicroscope.

Nitro blue tetrazolium Staining

Nitro blue tetrazolium (NBT) reacts with superoxide ions and forms formazan blue precipitate. This is visualized to identify superoxide production sites and to assess overall superoxide content in the tissue. Samples are stained in 0.1 mg/mL NBT and 0.05% (m/v) Tween™ 20 in 75 mM potassium phosphate buffer (pH 7.0) for 2 hours. After staining sample are treated in the same manner as described before (3:1:1 ac. acid, ethanol, glycerol 95°C 20 min) and observed with a Leica EZ4 W stereomicroscope after mounting on glass slide with the bleaching solution.

Results

1- Optimization of ROS measuring protocols in P. patens

1.1 stains

Trying to find a way to, at least, qualitatively assess the production and contents of ROS in tissue sample of *P. patens,* I tried to stain different mutants and wild type plants, exposed to different light and chemical stress, with dyes selective for superoxide ions or hydroperoxide molecules. I also tried some minor variant in bleaching conditions to eliminate endogenous pigments that would disrupt observation of the dye of interest.

The best conditions for bleaching tested: ethanol, acetic acid, glycerol in ratio 3:1:1 at 95°C for 20 minutes, this is sufficient to render both gametophores and protonema sample completely transparent. Stain results are of difficult interpretation for the intricate topology of the tissue and the tendency of protonema to collapse on itself, rendering difficult the formation of tissue monolayer on the microscopy slide. Despite the difficult observation, the stain procedures seem to work well enough to highlight some sub cellular compartment as main site of deposition of the insoluble products of the stain reactions. Specificity for super oxide and hydroxide species should be

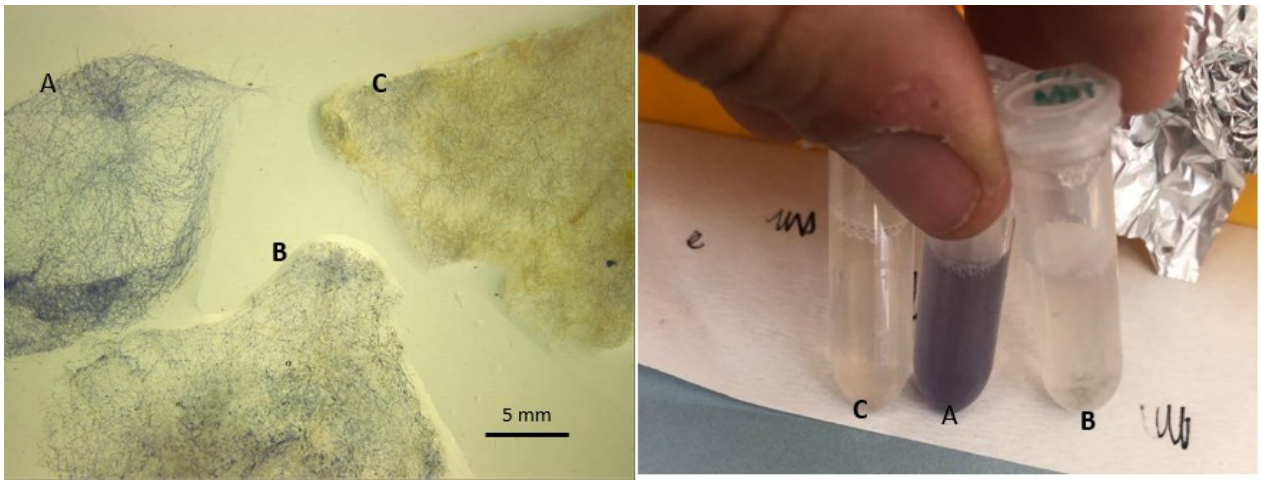

Figure 6: Nitro blue tetrazolium stained tissue (left) and staining solutions (right) of wt 2 weeks old plants adapted(1 week) to different light regimes A control light, B fluctuant light intensity, C high light.

confirmed with application of additional techniques. Strong conclusion on the overall ROS content of the tissue cannot be made but some differences between conditions can be observed (Figure 6).

In Figure 6 sample were grown for 1 week under control light intensity (50 umol photons\(m^2*s) 24h photoperiod) and then for 1 week under the selected light intensity (fluctuating light regime: alternate 1 min 125 umol photons\(m^2*s), 5 min 20 umol photons\(m^2*s), high light regime: 24h photoperiod 500 umol photons\(m^2*s)). The intensity in coloration of the control's staining solution respect to the high light and fluctuant light is remarkable. The difference in coloration intensity is less evident in plants acclimated for just 2 hours at the light conditions (Figure 7)

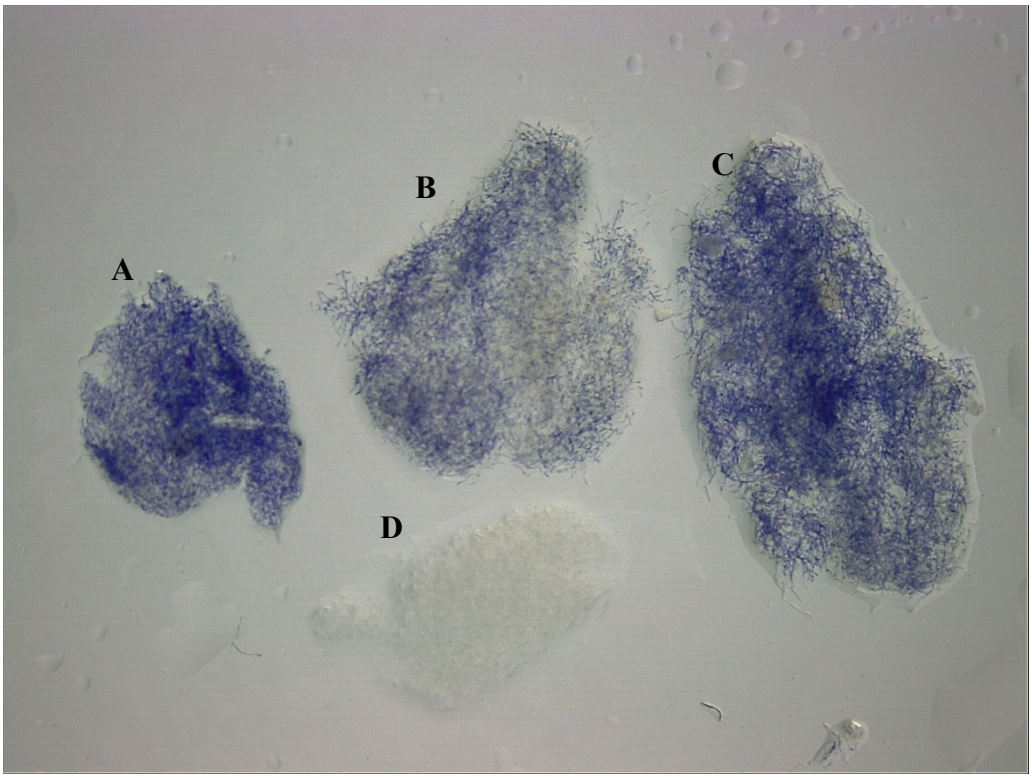

Figure 7: NBT stain (superoxide) of plant acclimated for 2 hours at: A control light, B High light, C fluctuating light. D non stained control sample.

1.2 colorimetric determination of hydrogen peroxide

Trying to obtain more precise and reproducible data on hydrogen peroxide contents of samples, Ferrous oxidation-xylenol orange assay was tested, this estimate the concentration of hydrogen peroxide in an aqueous extract of the sample analyzed.

My results on this assay are limited, some problem with plant growth that I have encountered during summer have limited the number of replicas.

From what I have observed, like many other assays for reactive oxygen species, results are heavily influenced by the conditions in which the assay is carried out. The species in analysis have limited half-life times and are easily degraded. The procedure is not robust and scalable enough to obtain the high number of replicas needed to confirm small changes in ROS contents.

In figure 8 the few data collected are presented, wtHL and *cox11HL* have been kept high light (HL) condition for 40 min prior the analysis. High light exposure in non-adapted plants correlate with a transient increase in ROS productions (Tripathy and Oelmüller, 2012) and so it is chosen to assess if any difference was detectable respect to plant kept at control light..

As is visible in figure 8, the data have broad distribution and the median value of the groups are very similar to each other without any trend for higher peroxide in plant exposed to higl light.

Also, the specificity of the assay is not been confirmed

All of this suggest that the FOX assays as implemented here is not to be informative

To assess the effects of light treatment on the contents of ROS in *P. patens* other assays must be tested and developed.

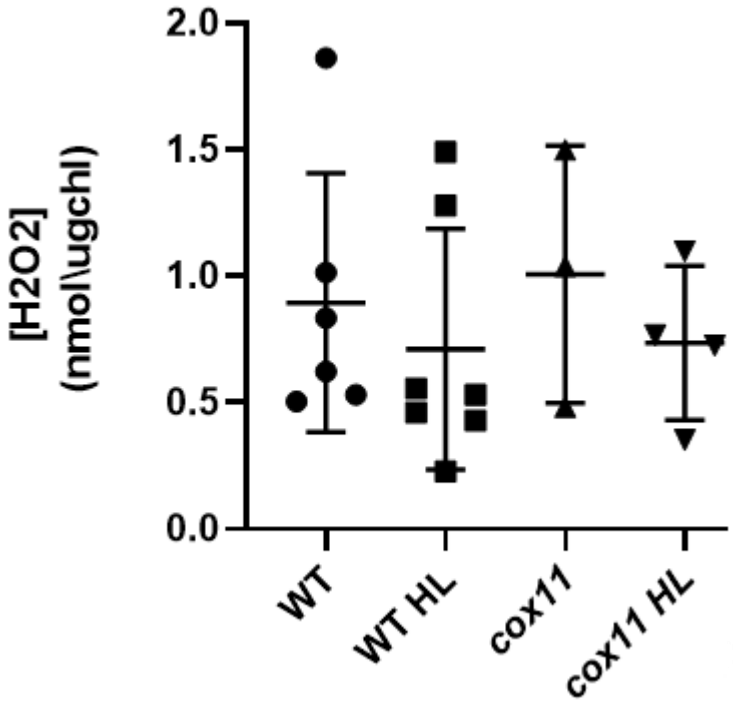

Figure 8: hydrogen peroxide concentration estimates by FOX assay of acqueus extracts of wild type and complex IV deficent lines. HL: high light

2- Respiratory characterization of *P. patens* WT and mutants

The second aim of this thesis was to assess the composition and capacity of the respiratory chain in different developmental stages and different mutants of *P. patens*.

To this aim, the respiratory rate of pieces of either protonema or gametophores was quantified in the presence or absence of the inhibitors KCN and SHAM (Figure 9). The effects on respiratory rate of the inhibitors on mutants (Figure 10) has been tested only on protonema since some mutants present impairment in gametophores production.

In addition to the experiments presented, replicas of the same procedure have been carried out using different inhibitor with the same targets of the one mentioned. The results reiterate the data presented, this confirm that observations are consequences of the inhibitions of the targeted enzymatic activity.

2.1. Comparison protonema-gametophore

The respiratory rate in the absence of inhibitors is not different between protonema and gametophores (1,5 pmolO_2\(s*mgChl)) . There is instead differences in the capacity of the Complex IV-mediated pathway.

In gametophore KCN alone causes the respiratory rate to drop significantly while SHAM seems to not produce effects, but to strongly affirm that more replicas should be obtained. (Figure 9)

To cause inhibition of respiration in protonema both inhibitors must be present at the same time, bringing the respiration rate of protonema to the same level of KCN inhibited gametophores. (Figure 9)

Overall, these data show differences in the respiratory functioning in the two studied developmental stages. In protonema both the complex IV and AOX pathways are ready to function, and both can accept electrons and transfer them to oxygen with the same capacity. Instead in gametophores, the AOX pathway doesn't show to be functioning, with a complete block of oxygen consumption when cyanide is present.

This suggests that gametophore doesn't utilize the non-energy conserving pathway nearly as much as protonema.

The difference between developmental stages could be due to the increased energy requirement of gametophores for the production of gametes. The AOX pathway dissipates the energy extracted from electrons as heat and is much less efficient than the complex IV pathway in conserving energy. Protonema is also the first tissue to develops and it must be able to deal with the stress of colonization and a range of conditions in which the presence and activity of AOX could be beneficial due the increased metabolic flexibility. For example in the case of temporary dessication with subsequent rehydration, a condition in which protonema stage is more likely to be, AOX could help with decreasing reoxigenation damage during the exit from hipoxic condition caused by the dissecation.(Jayawardhane *et al.*, 2020)

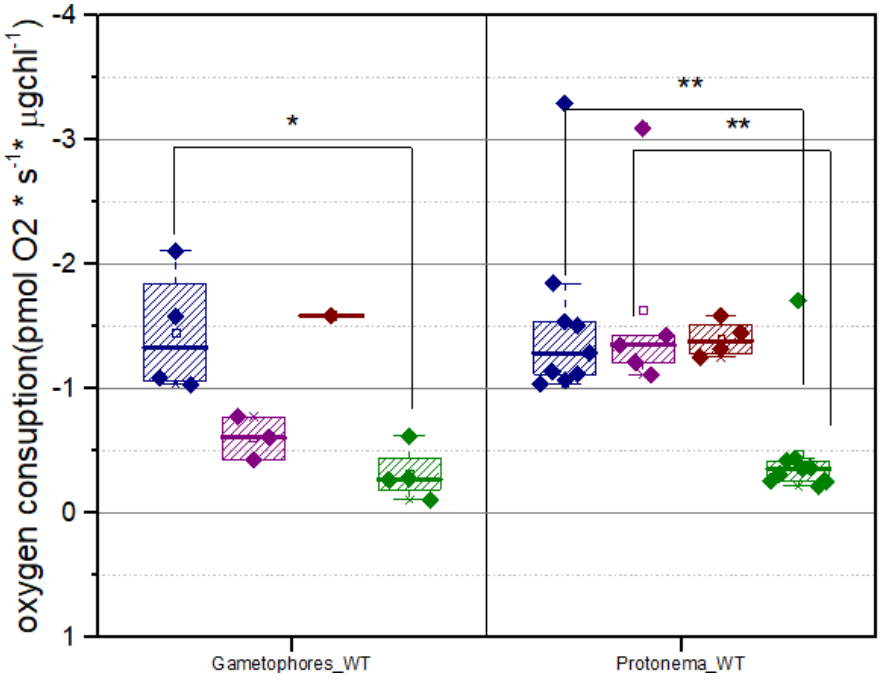

*Figure 9 respiration rate, normalized upon Chlorophyll content, of wild type Gametophores and protonema sample subjected to treatment with potassium cyanide or sham or both. Blue dots are single value for baseline respiration, purple are data for cyanide treatment, Red are data points for SHAM treatment and green represents the effects of application of both. Whisker and Box chart are presented for each data population, with thick line indication median value of the distribution and the box comprising data distributed between the 25% and 75% percentiles of the distribution. Asterisks represent the significance of pairwise comparisons (two sample t-test). (***=p<0.001 ; **=p<0.01 ; *=p<0.05)*

2.2. Respiratory characterization of cox11 and aox mutants

The respiratory functioning of two mutants of *P. patens* with altered levels of respiratory complexes previously isolated in the lab is tested. These lines are *cox11*, which is deficient in Complex IV activity, and *aox*, which is deficient in AOX activity. Since the developmental impairment of *cox11* plants abolishes the production of gametophores, I used protonema for all measurements. The protocol was the same reported in the previous section.

cox11 plants showed increased dark respiration in absence of inhibitors, almost twice the WT, from the 1,32 pmolO_2\(s*mgChl) of wild type to the 3,22 pmolO_2\(s*mgChl) of the mutant (figure 9 and 10). At first unexpected, since complex IV should be the main oxygen consumer, may be explained by the decreased number of protons translocated per oxygen molecule and the plant trying to compensate. KCN alone did not have an effect, as in WT. Importantly, **SHAM was capable of abolishing all respiration**, confirming that all O2 consumption was due to AOX.

aox mutants did not show differences in dark respiration in absence of inhibitors. KCN completely blocked respiration while SHAM doesn't have effects, confirming that CIV was responsible for all O2 consumption.

This shows that aox and cox11 are effectively depleted in AOX and CIV activities, respectively. Also, these experiments confirm that the concentrations of inhibitors used are sufficient to block their activities, and therefore they further verify that the absence of inhibition when KCN or SHAM were applied alone (Figure 9) was not due to technical reasons.

Wild type protonema sample show the same pattern of the data presented in the previous part. To observe a decrease in respiration is necessary both complex IV and AOX to be inhibited by the presence of both cyanide and SHAM.

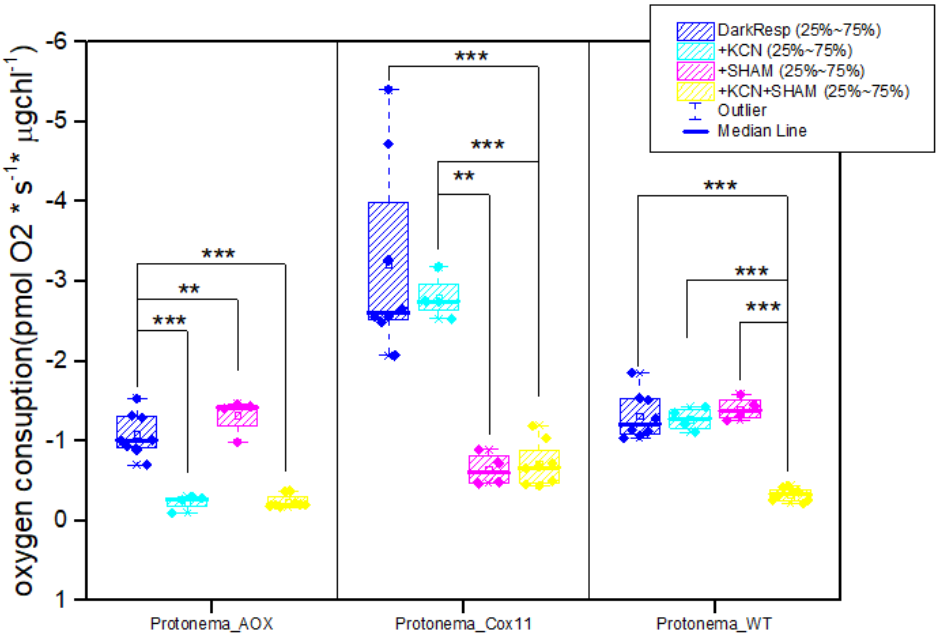

Figure 10: respiration rate, normalized upon Chlorophyll content, of protonema sample subjected to treatment with potassium cyanide or sham or both. DarkResp is the respiration rate of plant adapted for at least 40 min to dark before treatment.

Respiration of dark adapted ETC mutants

The respiration rate, in absence of inhibitors, of plant adapted to dark conditions have been measured for all the mETC mutants present in the lab (figure 11). This include also complex I ko mutants for which previous data have been published by our lab and in which some differences arise.

cox11 present an increase in respiration rate respect to the wt of around 2 times

aox present the same respiration rate as the wild type in dark adapted conditions

ndufa5 and *ndufb10* lines don't seem to present significant variation in respiration rate respect to the wt (figure 11), this is different from the result obtained by (Mellon *et al.*, 2021), in which an increase in oxygen consumption was reported

The results concerning *aox* and *cox11* are in line with the previous observations, instead concerning the results for complex 1 lines, those disagree with the results already published, in the previous work an increase in oxygen consumption rate was registered for both *ndufa5* and *ndufb10* lines. The differences could be explained by the low numer of replicas presented by me and in differences between experimental setups during data acquisition. This problem should be investigated further in my opinion.

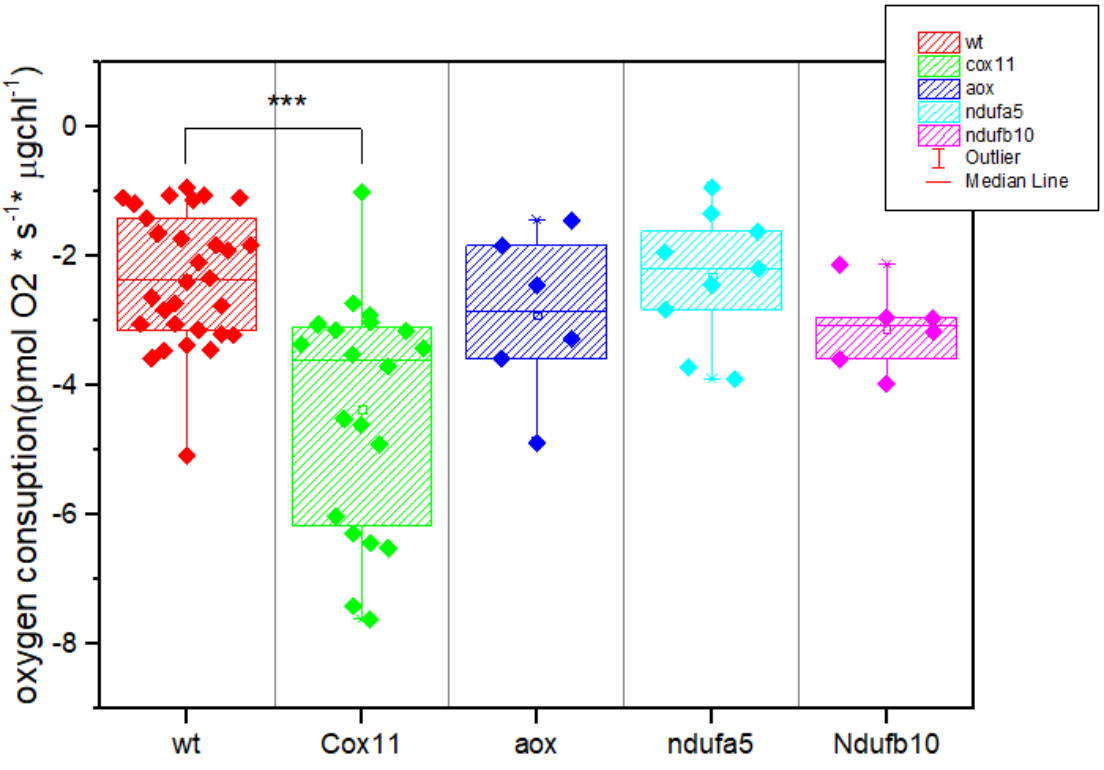

*Figure 11: respiration rate of wild type and ETC mutants protonema, Asterisks represent the significance. (***=p<0.001 ; **=p<0.01 ; *=p<0.05)statistical test :one way ANOVA.*

Cove, D. (2005) ‘The moss Physcomitrella patens’, *Annual Review of Genetics*, 39, pp. 339–358. Available at: https://doi.org/10.1146/annurev.genet.39.073003.110214.

Daudi, A. and O’Brien, J.A. (2012) ‘Detection of Hydrogen Peroxide by DAB Staining in’, *Bio-protocol*, 2(18), p. e263.

Fork, D.C. (1972) ‘Oxygen Electrode’, *Methods in Enzymology*, 24(C), pp. 113–122. Available at: https://doi.org/10.1016/0076-6879(72)24061-7.

Gu, L. (2023) ‘Optimizing the electron transport chain to sustainably improve photosynthesis’, *Plant Physiology*, pp. 1–15. Available at: https://doi.org/10.1093/plphys/kiad490.

Jayawardhane, J. *et al.* (2020) ‘Roles for Plant Mitochondrial Alternative Oxidase Under Normoxia, Hypoxia, and Reoxygenation Conditions’, *Frontiers in Plant Science*, 11(May). Available at: https://doi.org/10.3389/fpls.2020.00566.

Mellon, M. *et al.* (2021) ‘Inactivation of mitochondrial complex I stimulates chloroplast ATPase in Physcomitrium patens’, *Plant Physiology*, 187(2), pp. 931–946. Available at: https://doi.org/10.1093/plphys/kiab276.

Millar, A.H. *et al.* (2011) ‘Organization and regulation of mitochondrial respiration in plants’, *Annual Review of Plant Biology*, 62(May), pp. 79–104. Available at: https://doi.org/10.1146/annurev-arplant-042110-103857.

R.J. Porra, W.A.T.* and P.E.K.* and Dioision (1988) ‘Determination of accurate extinction coefficients and simultaneous equations for assaying chlorophylls a and b extracted with four different solvents: verification of the concentration of chlorophyll standards by atomic absorption spectroscopy’, *Biochimica et Biophysica Acta*, 975(3), pp. 384–394. Available at: https://doi.org/10.1213/ANE.0000000000001681.

Song, C. and Zhang, J. (2008) ‘PEM Fuel Cell Electrocatalysts and Catalyst Layers: Fundamentals and Applications. Electrocatalytic Oxygen Reduction Reaction’, pp. 89–134.

Tripathy, B.C. and Oelmüller, R. (2012) ‘Reactive oxygen species generation and signaling in plants’, *Plant Signaling and Behavior*, 7(12), pp. 1621–1633. Available at: https://doi.org/10.4161/psb.22455.

Zhang, Y. and Fernie, A.R. (2018) ‘On the role of the tricarboxylic acid cycle in plant productivity’, *Journal of Integrative Plant Biology*, 60(12), pp. 1199–1216. Available at: https://doi.org/10.1111/jipb.12690.

Zhu, X.G., Long, S.P. and Ort, D.R. (2010) ‘Improving photosynthetic efficiency for greater yield’, *Annual Review of Plant Biology*, 61, pp. 235–261. Available at: https://doi.org/10.1146/annurev-arplant-042809-112206.

1-(https://www.hamiltoncompany.com/process-analytics/dissolved-oxygen-knowledge/oxygen-measurement-principles/principles-of-polarographic-measurement)

2-(https://www.bioblast.at/index.php/Polarographic_oxygen_sensor)